Technical Report – SCEC award 20153 – Creating a multi-proxy approach to robustly capture earthquake temperature rise at the Punchbowl fault

PI - Alexis K. Ault (USU); Co-PIs - Heather Savage and Pratigya Polissar (UCSC)
Participants – Ema Armstrong (USU, MSc student), Kelly Bradbury (USU), Stuart Thomson (UA)

Objectives and significance for SCEC science goals

Intense friction-generated heat occurs along *thin, localized slip layers* during an earthquake. Heat facilitates dynamic fault weakening, rupture propagation, and transformation of the mechanical and chemical rock properties that influence subsequent deformation. However, documenting temperature rise in the rock record is challenging, as many chemical reactions are dependent on the magnitude and duration of heating. To address this science problem, we are directly comparing two different fault slip paleotemperature proxies: low-temperature thermochronometry (chiefly zircon (U-Th)/He (zircon He) thermochronometry) and thermal maturation of organic material (biomarkers) to quantify earthquake temperature rise in exhumed faults. We are applying high-spatial resolution zircon He thermochronometry to the well-characterized Punchbowl fault (PF), CA, and leveraging recent SCEC-supported biomarker data that demonstrates temperature rise occurred along localized principal slip zones (PSZs). Our research directly addresses the SCEC5 2020 Science Plan's research objectives:

- (Q3) *Structure, composition, and physical fault zone properties impact on resistance to seismic slip:* developing tools to link coseismic temperature rise and the width of the deforming fault zone informs the interplay between strain localization and slip velocity is seismogenic fault systems (**P3d**).
- (Q2) *Off-fault inelastic deformation impact on dynamic rupture and radiated seismic energy:* transient temperature rise and thermal decomposition weaken rocks and control dynamic rupture. Proposed high spatial resolution thermochronometric characterization of PF fault will inform how inelastic strain associated with evolving fault roughness and discontinuities influences earthquake physics (**P2d**).
- (Q1) *Fault loading across temporal and spatial scales:* coupled multi-scale fault textural observations and thermochronometry-based thermometry will map the 4D thermal evolution of the PF (**P1d**).

Work plan

Research team: consists of PI Ault (USU), an expert in fault rock thermochronometry and (U-Th)/He systematics; Co-PI Savage (UCSC), an expert in fault mechanics and fault paleotemperature proxies (Savage); and Co-PI Polissar, an expert in organic geochemistry. This project constitutes the MSc thesis research of USU graduate student Armstrong, and collaborators are Bradbury (USU), with expertise in structural and San Andreas fault geology and Thomson (UArizona) for apatite fission-track (AFT) analysis.

Division of work: Field work was carried by Armstrong, together with Ault and Bradbury in January 2020 and November 2020. Ault supervised Armstrong in thermochronometry sample processing, microscopy, and aliquot selection for (U-Th)/He and AFT analysis. Owing to COVID, Ault carried out (U-Th)/He analysis at UArizona and Thomson carried out AFT analyses. Savage mentored Armstrong on fault mechanics, and is assisting with comparison between existing biomarker results and new thermochronometry data, and thermal modeling. Co-PI Polissar will carry out organic molecule analysis at UCSC over the coming year.

Framework

Mapping past temperature rise from paleoearthquakes is critical for understanding fault mechanics, frictional energy dissipation, and slip histories, which in turn can inform future earthquake patterns (e.g., Rowe and Griffith, 2015). As an earthquake propagates, the active slipping zone is thought to localize from a thicker shear layer down to a millimeter-thick (or thinner) layer(s) (Rice, 2006; Platt et al., 2014; Rice et al., 2014; Platt et al., 2015). Such localization implies fault temperatures should increase dramatically due to frictional heating. Because pseudotachylyte (melted rock) is not ubiquitous in fault zones, prior work implied faults may not achieve temperatures much above ambient (Rice, 2006). However, recent SCEC-supported research developing sub-solidus thermometers, including organic biomarkers and hematite (U-Th)/He thermochronometry, has demonstrated that localized slip zones often experience temperature rise

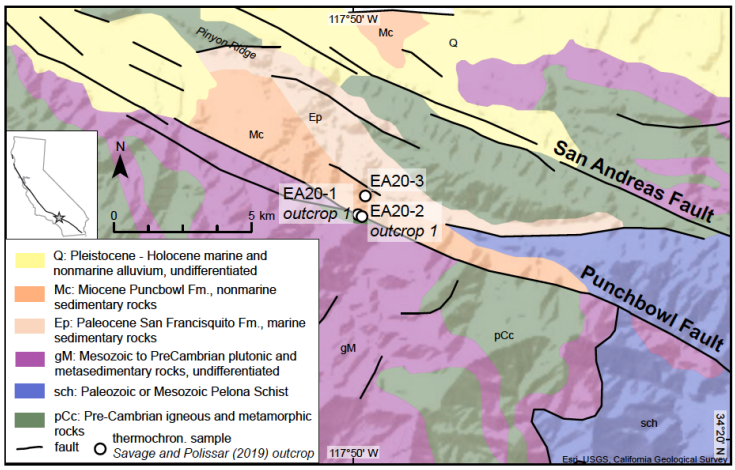

Figure 1. *Simplified geologic map of Devil's Punchbowl area showing sample locations to date.*

well above the background (Savage et al., 2014; Ault et al., 2015; Sheppard et al., 2015; McDermott et al., 2017; Rabinowitz et al., 2017; Coffey et al., 2019; Savage and Polissar, 2019; Calzolari et al., 2020).

This project compares biomarker data with (U-Th)/He thermochronometry of PSZs and ultracataclasite zones in the PF, an exhumed strand of the San Andreas fault system (Fig. 1). *To date, we have focused on the zircon He system.* Inter-method comparison of systems with different kinetics permits (***1***) proof-of-concept development of low-temperature thermochronometers as high-temperature thermometers, (***2***) temperature rise estimates for the PF, and (***3***) informs the interplay between strain localization, temperature rise, material property changes, and subsequent deformation.

Zircon (U-Th)/He thermochronometry quantifies the thermal evolution of rocks through time (Ault et al., 2019 and references within). The transition between open and closed system behavior, characterized by He retention, is known as the closure temperature (T_c) (Dodson, 1973). The T_c of the zircon He system is ~200-25 °C (10 °C/Myr cooling rate). He loss is influenced by zircon radiation damage from actinide decay. Assuming a population of grains experienced the same thermal history, eU ([U]+0.235*[Th]) is proportional to accumulated damage (Guenthner et al., 2013). Damage accumulation results in progressive crystal "metamictization" (Holland and Gottfried, 1955; Nasdala et al., 1995; Nasdala et al., 2001). Metamictization is visible in plane polarized light with a stereoscope: undamaged, low eU zircons are transparent; high eU, metamict zircons are brown-black and opaque (Ewing et al., 2003; Ault et al., 2018). Damage initially impedes He diffusion, increases T_c, and yields older dates. With increasing accumulation, damage becomes interconnected, diffusivity increases, and T_c and date decrease (Guenthner et al., 2013). Samples that experience slow cooling, prolonged residence in the He partial retention zone, and(or) reheating may yield positive and(or) negative relationships between zircon He date and eU, that can be leveraged to reconstruct a samples' thermal history (Guenthner et al., 2013; Orme et al., 2016; Guenthner et al., 2017; Johnson et al., 2017; Ault et al., 2018). He diffusion kinetics also respond to short duration, high temperature thermal pulses (e.g., Murakami et al., 2006; Tagami, 2012; Ault et al., 2015; McDermott et al., 2017) associated with frictional heating in either a bulk layer or concentrated as asperities (Archard, 1959; Rice, 2006; Ben-Zion and Sammis, 2013; Proctor et al., 2014; Sleep, 2019).

Research progress to date

1. Field work, sampling approach, and analytical methods

Samples were collected in Devil's Punchbowl Park, CA, where semi-continuous exposures of the Punchbowl fault (PF) are preserved (Fig. 1). To date, sample locations replicate two locations that are part of *Outcrop 1* of Savage and Polissar (2019), which exhibited biomarker evidence for increased temperature rise along the principal slip zone (PSZ). Here, two high-spatial resolution transects perpendicular to the trace of the PF are separated by ~10 m along strike (sites EA20-1 and EA20-2). At each site, we collected crystalline basement, Punchbowl Formation (Fm.), and PF gouge over a distance of a ~10 cm (Fig. 2). Gouge domains are comminuted and friable. Individual layers of the gouge were isolated with a knife and collected with a flat trowel. We also sampled undeformed Punchbowl Fm. ~100 m north of the PF.

The structural architecture of the gouge is distinct at each site. At EA20-1, we sub-sampled the gouge based on prior characterization (Chester and Chester, 1998; Savage and Polissar, 2019) because sub-

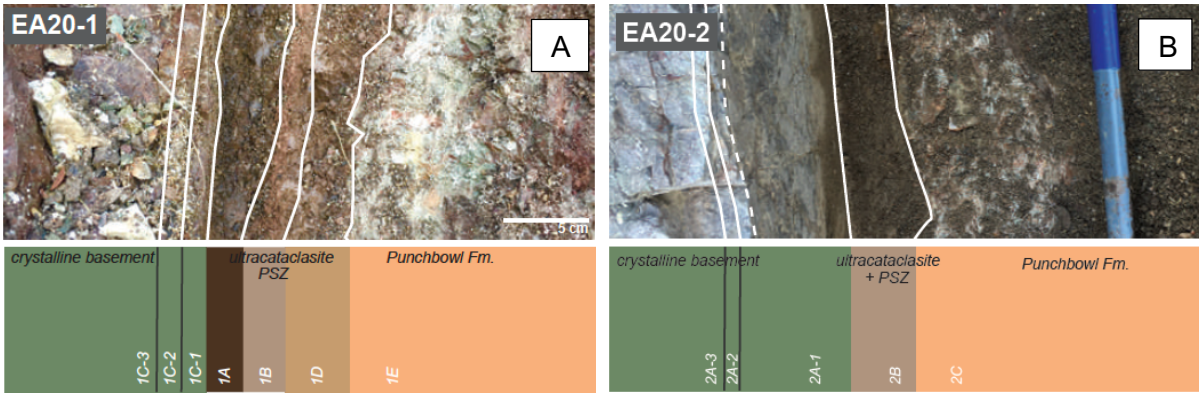

Figure 2. *Field photographs from sites EA20-1 (left) and EA20-2 (right). White lines and underlying schematics highlight fault zone architecture and sample IDs at each site.*

units could be distinguished by color (Fig. 2A). Gouge domains include: basement-side (black) ultracataclasite, PSZ fault gouge, and Punchbowl formation-side (brown) ultracataclasite. The gouge at site EA20-2 is comparatively homogeneous and lacked obvious sub-domains, so we acquired a single gouge sample (Fig. 2B). Crystalline basement samples were subsequently slabbed with a water-cooled saw perpendicular to the gouge contact at 1-cm intervals to create subsamples away from the gouge interface.

Accessory phases were isolated using standard crushing methods including mortar and pestle for more friable samples, and magnetic and density separation techniques in the USU Mineral Microscopy and Separation Lab (M^2SL). Whole zircon grains and apatite fragments were present in each sample, but whole apatite grains were only present in the Punchbowl Fm. sample EA20-3A. We targeted a subset of samples for thermochronometry including the PSZ (1B), gouge (2B), basement (1C-1, 1C-3, 2A-1, 2A-3), and Punchbowl Fm. (1E, 3A) because of inferences about the presence and absence of friction-generated heat based on biomarker data (Savage and Polissar, 2019). Zircon grains were selected following the approach of Ault et al. (2018) to encapsulate the range of visual metamictization in each sample.

Target zircon and apatite grains were imaged, measured using a stereoscope and Leica software, and loaded into 1 mm Nb tubes in the M^2SL. Grains were analyzed for U, Th, Sm (apatite only) and He at University of Arizona's Arizona Radiogenic Helium Dating Lab (ARHDL) following standard apatite and zircon degassing, spiking, and dissolution protocols. Apatite fragments from a subset of samples were analyzed for apatite fission-track (AFT) thermochronometry at the Arizona FT Lab.

2. Thermochronometry results

To date, we have acquired 45 individual zircon He dates from eight samples. Based on the observed range of zircon textures and morphology of each of our mineral separates, most grains selected for zircon He analysis are clear/transparent and faceted, although some grains are honey brown/translucent (e.g., Fig. 3A inset). Most grains have low eU (<500 ppm), implying they have low accumulated radiation damage (Fig. 3A). Limited intra- and inter-sample eU variability make it difficult to evaluate demonstrable relationships between visual metamictization and eU concentration.

Figure 3A depicts individual zircon He dates, classified by sample, as a function of eU. Individual zircon He dates from basement samples range from ~11 Ma to ~29 Ma over a restricted eU range of 97-386 ppm. Punchbowl Fm. samples yield individual zircon He dates of ~21-64 Ma over 182-1945 ppm eU. PSZ (sample 1B) and gouge (sample 2B) dates are ~17 Ma to ~84 Ma over an eU of 345-1102 ppm. Apatite (U-Th)/He (apatite He) and AFT thermochronometry provide a comparison to our zircon He results. Only Punchbowl Fm. sample 3A contained apatite suitable for (U-Th)/He analysis. Individual apatite He dates from this sample are ~4 Ma, and are uniform over a broad 17-157 ppm eU range (Fig. 3B). Fragments analyzed for AFT are plagued by minimal tracks, resulting in large individual and sample-level uncertainties. Eight preliminary AFT dates range from ~9 Ma to 25 Ma.

3. Preliminary interpretations

The majority of targeted zircon crystals are fairly pristine (e.g., inset in Fig. 3A; cf. Ault et al., 2018 and metamict grains from Archean and Paleoproterozoic samples). The commensurate low eU concentration,

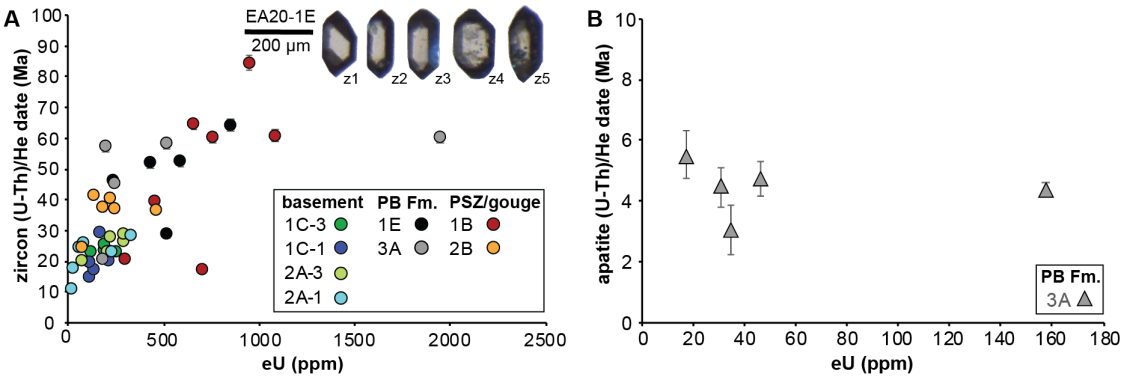

Figure 3. *Individual (A) zircon and (B) apatite (U-Th)/He dates as a function of eU. Dated plotted with 2σ analytical uncertainties. PSZ = principal slip zones; PB Fm. = Punchbowl Formation. Inset in A shows photographs of analyzed zircon crystals from sample 1E.*

together with the likely Phanerozoic crystallization age for detrital zircons from the Punchbowl Fm. and potential Mesozoic crystallization age for the crystalline basement zircon, means that analyzed grains have net low accumulated radiation damage. Thus, samples from sites 1 and 2 (outcrop 1 of Savage and Polissar, 2019) did not yield metamict, high radiation-damage zircon crystals, which are most amenable to thermal resetting (i.e., He loss) from short duration, high-temperature frictional heating.

Zircon He data from all samples collectively define a positive zircon He date-eU trend with dates plateauing at ~60 Ma (Fig. 3A). With the exception of one outlier in sample 1B, zircon He dates from the PSZ at site 1 and gouge at site 2 do not deviate from this pattern. Punchbowl Fm. apatite He data away from the PF support rapid cooling at ~4 Ma because dates are uniform across a broad eU range. Assuming this phase of exhumation is related to fault slip, our data may represent the best new constraint on the timing of PF activity. We note the youngest zircon He date associated with the lowest eU grain does not overlap with the apatite He data (Fig. 3). Together with the positive zircon He date-eU trend, these observations suggest that, to first order, zircon He data patterns from sites 1 and 2 likely reflect the long-term thermal history as opposed to coseismic temperature rise.

On-going and future work

On-going research is aimed at (***1***) comparing zircon He data with existing biomarker data (Savage and Polissar, 2019) via suites of numerical models, and (***2***) acquisition of low-temperature thermochronometry data from outcrop 2 of Savage and Polissar (2019), and (***3***) new biomarker measurements from existing samples. The evolving COVID-19 pandemic, as well as the Bobcat fire that swept through and shuttered Devil's Punchbowl Natural Area, have resulted in research delays and the project timeline has been extended through 01/31/2022 to allow for completion of project goals.

Prior biomarker thermometry on the PF supports structural observations that PSZs within the fault core hosted earthquake slip and validates biomarker method systematics (Chester and Chester 1998; Savage and Polissar, 2019). In addition to the PSZ, one type of ultracataclasite within the fault zone also appears to be thermally-altered, supporting the idea that it is composed of past localized slip zones that achieved temperature rise between 464-1062 °C (Chester and Chester 1998; Savage and Polissar, 2019). The lack of evidence for thermal resetting from our zircon He results at outcrop 1 of Savage and Polissar (2019) implies that coseismic temperatures may have been at the lower end of this spectrum based on models of biomarker results. Armstrong, supervised by Ault, is currently modeling paired coseismic temperature rise (Lachenbruch, 1986) with fractional He loss for a range of variably-damaged zircon (Table 4 in Guenthner et al., 2013) to further evaluate this. On-going modeling using the software HeFTy (Ketcham, 2005) is leveraging the positive zircon He date-eU pattern to reconstruct the long-term thermal history. Temperature rise was likely not continuous along the fault, even within ~1 m from spots that showed an increase in thermal maturity in the PSZ (Savage and Polissar, 2019). Thus, we will also analyze new samples collected in Jan. 2020 for biomarker data for comparison with existing zircon He data (Polissar et al., 2011; Sheppard et al., 2015). We also plan to sample outcrop 2 of Savage and Polissar (2019) because this site yields the highest MPI-4 index in the PSZ and the highest inferred fault slip temperatures.

References

Archard, J.F., 1959, The temperature of rubbing surfaces: Wear, v. 2, p. 438-55.

Ault, A.K., Gautheron, C., and King, G.E., 2019, Innovations in (U-Th)/He, fission-track, and trapped-charge thermochronometry with applications to earthquakes, weathering, surface-mantle connections, and the growth and decay of mountains: Tectonics, Grand Challenges in the Earth and Space Sciences, Centenniel Collection, v. 38, p. 3705-3739.

Ault, A.K., Guenthner, W.R., Moser, A.C., Miller, G.H., and Refsnider, K.A., 2018, Zircon selection reveals (de)coupled zircon metamictization, radiation damage, and He diffusivity: Chemical Geology, v. 490, p. 1-12.

Ault, A.K., Reiners, P.W., Evans, J.P., and Thomson, S.N., 2015, Linking hematite (U-Th)/He dating with the microtextural record of seismicity in the Wasatch fault damage zone, Utah, USA: Geology, v. 43, p. 771-774.

Ben-Zion, Y., and Sammis, C.G., 2013, Shear heating during distributed fracturing and pulverization of rocks: Geology, v. 41, p. 139-142.

Calzolari, G., Ault, A.K., Hirth, G., and McDermott, R.G., 2020, Hematite (U-Th)/He thermochronometry detects asperity flash heating during laboratory earthquakes: Geology, v. 48, p. 514-518.

Chester, F.M., and Chester, J.S., 1998, Ultracataclasite structure and friction processes of the Punchbowl fault, San Andreas system, California: Tectonophysics, v. 295, p. 199-221.

Coffey, G.L., Savage, H.M., Polissar, P.J., Rowe, C.D., and Rabinowitz, H.S., 2019, Hot on the trail: Coseismic heating on a localized structure along the Muddy Mountain fault, Nevada: Journal of Structural Geology, v. 120, p. 67-79.

Dodson, M.H., 1973, Closure temperatures in cooling geological and petrological systems: Contributions to Mineralogy and Petrology, v. 40, p. 259-274.

Ewing, R.C., Meldrum, A., Wang, L., Weber, W.J., and Rene Corrales, L., 2003, Radiation effects in zircon: Reviews in Mineralogy and Geochemistry, v. 53, p. 387-425.

Guenthner, W.R., Reiners, P.W., Drake, H., and Tillberg, M., 2017, Zircon, titanite, and apatite (U-Th)/He ages and age-eU correlatiions from the Fennoscandian Shield, southern Sweden: Tectonics, v. 36, p. 1-21.

Guenthner, W.R., Reiners, P.W., Ketcham, R.A., Nasdala, L., and Giester, G., 2013, Helium diffusion in natural zircon: radiation damage, anisotropy, and the interpretation of zircon (U-Th)/He thermochronology: American Journal of Science, v. 313, p. 145-198.

Holland, H.D., and Gottfried, D., 1955, The effect of nuclear radiation on the structure of zircon: Acta Crystallographica, v. 8, p. 291-300.

Johnson, J.E., Flowers, R.M., Baird, G.B., and Mahan, K.H., 2017, "Inverted" zircon and apatite (U-Th)/He dates from the Front Range, Colorado: High-damage zircon as a low-temperature (< 50 °C) thermochronometer": Earth and Planetary Science Letters, v. 466, p. 80-90.

Ketcham, R.A., 2005, Forward and inverse modeling of low-temperature thermochronometry data: Reviews in Mineralogy and Geochemistry, v. 58, p. 275-314.

Lachenbruch, A.H., 1986, Simple models for the estimation and measurement of frictional heating by an earthquake: U.S. Geological Survey Open File Report 86-508, p. 13 p.

McDermott, R.G., Ault, A.K., Evans, J.P., and Reiners, P.W., 2017, Thermochronometric and textural evidence for seismicity via asperity flash heating on exhumed hematite fault mirrors, Wasatch fault zone, UT, USA: Earth and Planetary Science Letters, v. 471, p. 85-93.

Murakami, M., Yamada, R., and Tagami, T., 2006, Short-term annealing characteristics of spontaneous fission tracks in zircon: A qualitative description: Chemical geology, v. 227, p. 214-222.

Nasdala, L., Irmer, G., and Wolf, D., 1995, The degree of metamictization in zircon: A Raman spectroscopic study: European Journal of Mineralogy, v. 7, p. 471-478.

Nasdala, L., Wenzel, M., Vavra, G., Irmer, G., Wenzel, T., and Kober, B., 2001, Metamictisation of natural zircon: accumulation versus thermal annealing of radioactivity-induced damage: Contributions to Mineralogy and Petrology, v. 141, p. 125-144.

Orme, D.A., Guenthner, W.R., Laskowski, A.K., and Reiners, P.W., 2016, Long-term tectonothermal history of Laramide basement from zircon-He age-eU correlations: Earth and Planetary Science Letters, v. 453, p. 119-130.

Platt, J.D., Brantut, N., and Rice, J.R., 2015, Strain localization driven by thermal decomposition during seismic shear: Journal of Geophysical Research: Solid Earth, v. 120, p. 4405-4433.

Platt, J.D., Rudnicki, J.W., and Rice, J.R., 2014, Stability and localization of rapid shear in fluid-saturated fault gouge: 2. Localized zone width and strength evolution: Journal of Geophysical Research: Solid Earth, v. 119, p. 4334-4359.

Polissar, P.J., Savage, H.M., and Brodsky, E.E., 2011, Extractable organic material in fault zones as a tool to investidate frictional stress: Earth and Planetary Science Letters, v. 311, p. 439-447.

Proctor, B.P., Mitchell, R.H., Hirth, G., Goldsby, D.L., Zorzi, F., Platt, J.D., and Di Toro, G., 2014, Dynamic weakening of serpentinite gouges and bare surfaces at seismic slip rates.: Journal of Geophysical Research Solid Earth, v. 119, p. 8107-8131.

Rabinowitz, H.S., Polissar, P.J., and Savage, H.M., 2017, Reaction kinetics of alkenone and n-alkane thermal alteration at seismic timescales: Geochemistry, Geophysics, Geosystems, v. 18, p. 204-219.

Rice, J.R., 2006, Heating and weakening of faults during earthquake slip: Journal of Geophysical Research, v. 111, p. B05311.

Rice, J.R., Rudnicki, J.W., and Platt, J.D., 2014, Stability and localization of rapid shear in fluid-saturated fault gouge: 1. Linearized stability analysis: Journal of Geophysical Research: Solid Earth, v. 119, p. 4311-4333.

Rowe, C.D., and Griffith, W.A., 2015, Do faults preserve a record of seismic slip: a second opinion: Journal of Structural Geology, v. 78, p. 1-26.

Savage, H.M., and Polissar, P.J., 2019, Biomarker thermal maturity reveals localized temperature rise from paleoseismic slip along the punchbowl fault, CA, USA: Geochemistry, Geophysics, Geosystems, v. 20, p. 3201-3215.

Savage, H.M., Polissar, P.J., Sheppard, R.E., Rowe, C.D., and Brodsky, E.E., 2014, Biomarkers heat up during earthquakes: New evidence of seismic slip in the rock record: Geology, v. 42, p. 99-102.

Sheppard, R.E., Polissar, P.J., and Savage, H.M., 2015, Organic thermal maturity as a proxy for frictional fault heating: Experimental constraints on methylphenanthrene kinetics at earthquake timescales: Geochimica et Cosmochimica Acta, v. 151, p. 103-116.

Sleep, N.H., 2019, Thermal weakening of asperity tips on fault planes at high sliding velocities: Geochemistry, Geophysics, Geosystems, v. 20, p. 1164-1188.

Tagami, T., 2012, Thermochronological investigations of fault zones: Tectonophysics, v. 538-540, p. 67-85.